A Triggerless readout system for the ANDA electromagnetic calorimeter

Tiemens, M.

Published in:
Journal of Physics: Conference Series

DOI:
10.1088/1742-6596/587/1/012025

Publication date:
2015

A Triggerless readout system for the $\bar{P}ANDA$ electromagnetic calorimeter

Journal of Physics: Conference Series **587** (2015) 012025 doi:10.1088/1742-6596/587/1/012025

A Triggerless readout system for the $\bar{P}ANDA$ electromagnetic calorimeter

M. Tiemens on behalf of the PANDA Collaboration

KVI - Center For Advanced Radiation Technology, University of Groningen, Zernikelaan 25, 9747 AA Groningen, The Netherlands

E-mail: m.tiemens@rug.nl

Abstract. One of the physics goals of the future $\bar{P}ANDA$ experiment at FAIR is to research newly discovered exotic states. Because the detector response created by these particles is very similar to the background channels, a new type of data readout had to be developed, called "triggerless" readout. In this concept, each detector subsystem preprocesses the signal, so that in a later stage, high-level phyiscs constraints can be applied to select events of interest. A dedicated clock source using a protocol called SODANET over optical fibers ensures proper synchronisation between the components. For this new type of readout, a new way of simulating the detector response also needed to be developed, taking into account the effects of pile-up caused by the 20 MHz interaction rate.

1. Introduction

A new experiment is being developed to perform precision measurements in the energy range between 1.7 and 5.5 GeV, where Quantum Chromodynamics becomes non-perturbative for charmonium systems[1]. The experiment is called $\bar{P}ANDA$ ($\bar{P}$ ANnihilations at DArmstadt), and one of the mysteries that it hopes to unravel is the generation of hadron masses, as for these composite particles, the sum of the parts does not add up to the whole (in fact, for e.g. protons, the sum of the valence quark masses only adds up to about 1% of the proton mass [1]). Furthermore, over the last years, several new charmonium-like hadrons were discovered, called XYZ states [2], possibly consisting of more than 3 quarks. $\bar{P}ANDA$ will be able to perform precision measurements on the properties of these and other predicted, as-of-yet unobserved (such as glueballs), exotic states of matter, which can be directly populated through the proton-antiproton interactions.

The $\bar{P}ANDA$ experiment will be build at the new Facility for Antiproton and Ion Research (FAIR), currently under construction in Darmstadt, Germany. FAIR's main accelerator will be used to create an antiproton beam, which will be stored in the High Energy Storage Ring (HESR). The $\bar{P}ANDA$ experiment will be placed inside the HESR. The antiproton beam impinges on a proton target, made of frozen hydrogen pallets [3]. In these so-called fixed-target experiments, particle production will be forward boosted, leading to an asymmetric detector design, see Figure 1. The $\bar{P}ANDA$ detector will follow the "traditional" onion-like design, where the detector subsystems are placed nested in each other to be able to measure all the properties

[1] Charmonium is the bound state of a charm and an anticharm quark

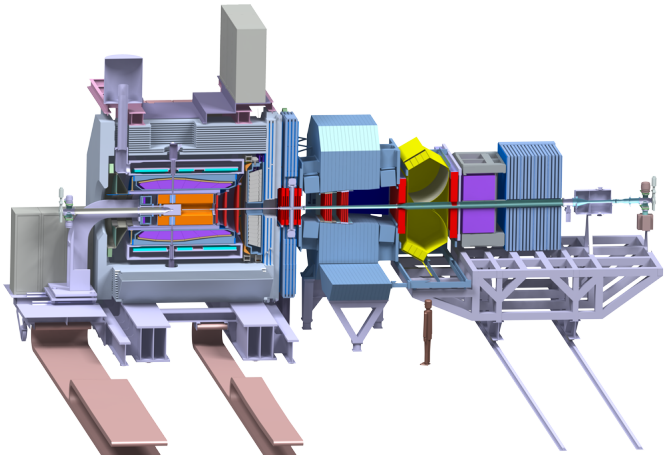

Figure 1. CATIA drawing of the $\bar{P}ANDA$ detector. *Courtesy:* A. Cebulla, FZ Juelich, 2014.

of the particles produced in the annihilations. This paper will mainly focus on one subsystem, the electromagnetic calorimeter (EMC). The scintillation crystals are made of second generation lead tungstate ($PbWO_4$, PWO), featuring an improved light yield over first generation PWO by a factor 2. The crystals are cooled down to -25 ℃, improving the light yield by another factor 2. This will enable an energy resolution of 1% at 1 GeV. The crystals will be 20 cm long, which is estimated to be about 22 radiation lengths, with the front and back face about 2×2 cm. The complete EMC consists of three parts: a Barrel, containing 11,360 scintillation crystals and a Backward and Forward Endcap, containing 528 and 3856 crystals, respectively.

2. The readout of the detector

Traditionally, the data stream being produced is reduced using hardware triggers, based on the topology of the response in one of the detector subsystems. However, for $\bar{P}ANDA$, this approach is insufficient. The reason for this, is that there are many background channels with a similar final-state topology as the decays of interest. A typical example is the decay of a recently discovered exotic state candidate, the $Y(4260)$. A strong decay mode is through a J/ψ particle and two neutral pions. Prominent final-state products of these particles feature an electron-positron pair and 4 photons, respectively:

$$p\bar{p} \to Y(4260) \to J/\psi\pi^0\pi^0 \to e^+e^- + 4\gamma$$

However, there are many decay modes with a similar final-state topology, some examples of which are shown here:

$$p\bar{p} \to J/\psi\eta\eta \to e^+e^- + 4\gamma,$$
$$p\bar{p} \to J/\psi\eta\pi^0 \to e^+e^- + 4\gamma,$$
$$p\bar{p} \to J/\psi\pi^+\pi^-\pi^0\pi^0 \to e^+e^- + 4\gamma.$$

The presence of this large number of background channels with a similar final-state topology renders the triggered readout unusable, since the hardware triggers, which in this case will be based on final-state photon multiplicities, will allow events from these background channels to pass, so a sufficient reduction factor cannot be achieved when searching for $Y(4260)$ events.

2.1. Solution

The proposed solution for $\bar{P}ANDA$ is to reconstruct events in realtime during data taking, after which high-level physics-inspired constraints can be imposed to perform event selection before sending data to storage. In the previous example, taking the invariant mass of the final state particles into account allows to distinguish between the desired signal and the one generated by background events. To illustrate this, the concept of this "triggerless" readout of the detector will be explored below for the EMC.

3. The readout chain for the EMC

For the $\bar{P}ANDA$ EMC, the readout chain can be divided into *five parts*:

- The front-end electronics, consisting of *photosensors, preamplifiers,* and *digitisation modules*. These are placed inside the detector, and will therefore be exposed to high levels of radiation.
- An intelligent, self-triggering, dead-time-free readout, starting with the *digitisation modules*, and including *data concentrators* and *compute nodes*. The data concentrators and compute nodes are placed outside the detector. Data will be transported from the digitisation modules using high-speed (5 Gbps) optical links.

3.1. Photosensors

For the EMC, the readout starts with the photosensors. Two types will be used:

- Hamamatsu Silicon Avalanche Photo Diodes (APDs). These feature a high quantum efficiency in the order of 70-80%. These are large area APDs, with an active area of 7×14 mm, two of which will be fitted to each crystal to cover most of the back face. This increases the light collection, offers redundancy (see Section 3.4) and allows the detection of a nuclear counter event.
- Hamamatsu Vacuum Photo Tetrodes (VPTTs). The quantum efficiency for these is around 20%. VPTTs are radiation hard and can handle high hit rates, and will therefore be used in the most forward region of the EMC (i.e. at the centre of the Forward Endcap). One VPTT is needed for each crystal.

3.2. Preamplifiers

The preamplifiers have been discussed in detail by I. Keshelashvili, see [4]. See also [5] for the second type of preamplifier (the APFEL ASIC) that will be used in the $\bar{P}ANDA$ experiment.

3.3. Digitisers

After the preamplifiers, the signal is fed to a 64-channel, 14-bit Sampling Analogue-to-Digital Converter (SADC), which continuously digitises the input signal at a rate of 80 MHz. Since each APFEL preamplifier offers two outputs, and the LNP preamplifiers feature a dedicated splitter, addressing inputs with two different gains on the digitisers, every digitiser can read out 32 photosensors. The hardware design of this device was made by P. Marciniewski, and the firmware was developed at KVI-CART [6].

After the digitisation stage, two Xilinx Kintex-7 Field-Programmable Gate Arrays (FPGAs), a chip with fully programmable logic blocks for fast, task-specific calculations, are used to perform preprocessing of the signal. First, DC offsets in the baseline of the signal are corrected for, so all amplitudes are measured with respect to the same reference point. The next stage is pulse detection. If the amplitude of a pulse crosses a set threshold, a discrimination is made between single or so-called pile-up pulses. A pile-up of pulses occurs when a second particle hits

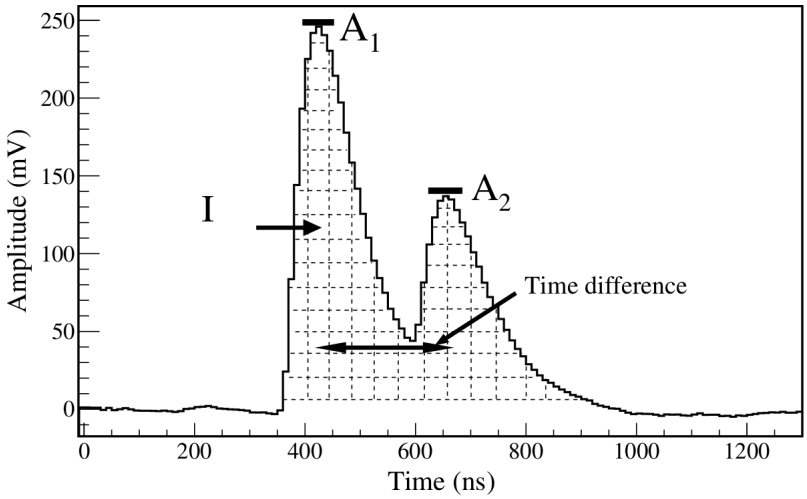

Figure 2. A typical pile-up pulse (after digitisation) [8]. The symbols are explained in the text.

the detector within the response time, superimposing the second pulse on the first (see Figure 2). For an interaction rate of 20 MHz, assuming a Poisson distribution of events, the probability for a pile-up to occur is about 9%, and for multiple pile-up, it is less than 0.5%. The digitiser discriminates by considering the ratio between the amplitude and the area [7, 8] of the peak, whose relation[2] is given by:

$$I = k(A_1 + A_2), \tag{1}$$

where I is the area of the waveform, k a constant to be determined by calibration, and A_1 and A_2 the amplitude of the first and the second peak, respectively. Rewriting this into a ratio (taking the ratio with the amplitude of the first pulse):

$$I/A_1 = k(1 + A_2/A_1), \tag{2}$$

if A_2 is zero (i.e., no pile-up pulse), $I/A_1 = k$, therefore by setting a threshold for the ratio, it is possible to discriminate between the two cases. In Figure 3, a measurement on this ratio performed by G. Tambave *et al* [7] is shown.

If a pile-up pulse is identified, the complete waveform is sent to the data concentrators. If a single pulse was detected, the amplitude of the pulse, being a measure for the energy deposited in the crystal, is extracted, and the associated timestamp is calculated using Constant Fraction Discrimination. Finally, only this information is sent on to the next stage. This process is called "Feature Extraction".

Some additional features of the SADCs include:

- A compact design (160×100 mm), which is needed due to space restrictions in the detector volume.
- Advanced debugging capabilities, including the possibility to read out the baseline and complete waveform of pulses.
- Fast rebooting (a few milliseconds) after radiation damage to the device's configuration register is detected.

[2] This relation only holds if the pulse shape is stable, which was found to be the case [7]

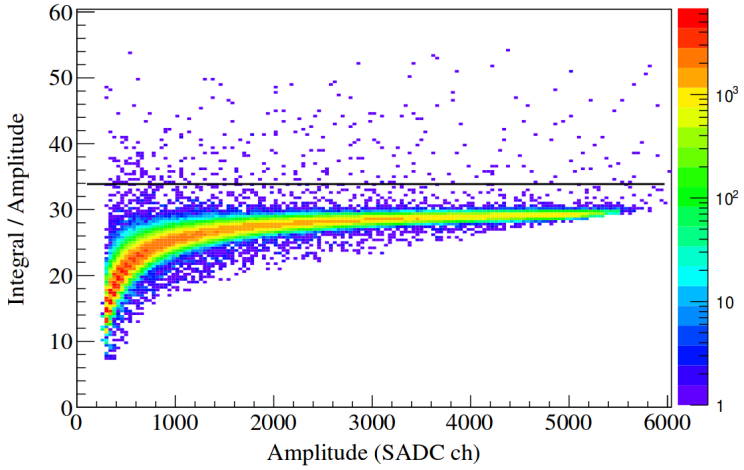

Figure 3. The offline calculated I/A ratio. The majority of points (coming from the more common single pulses) lie at a line equal to $I/A = k$, allowing to set the black horizontal line as a threshold for discriminating pile-up pulses (at 3σ significance above k).

3.4. Data Concentration

The next stage in the readout chain are the data concentrators, whose current hardware is based on TRBv3 developed at GSI [9]. For redundancy, each APD of a crystal will be read out by a separate digitiser, therefore, if one of the digitisers ceases to function, it is still possible to read out the crystals connected to this digitiser. By recombining this information, the amount of data can be reduced.

3.4.1. Pile-up Recovery The data concentrators feature a recovery algorithm for the pile-up pulses being sent from the digitisers[3] [8]. The algorithm is inspired by Eq. (2). From the calibration to single pulses, the constant k can be determined, and the total integral I and amplitude A_1 of the first pulse can be obtained from the waveform. A_1 can be determined unambiguously if the second pulse comes after the rise time of about 50 ns, as then, it won't affect the amplitude of the first pulse. The amplitude A_2 of the pile-up pulse then follows directly from Eq. (2), since all other parameters are determined. To test this procedure, an experiment was performed with a tagged photon beam in MAMI, Mainz [7]. The amplitude recovery was tested by taking the amplitude of the first pulse as A_1 and recovering the amplitude of the second (left picture in Figure 4), and by taking the amplitude of the second pulse as A_1 and recovering the first (right picture in Figure 4). From the FWHM of the recovered pulses, Figure 4 shows that in both cases it is possible to recover the amplitude of the other pulse, showing the viability of the method.

3.4.2. Synchronisation In experiments using a hardware trigger, the synchronisation between the different parts of the detector is also automatically provided by the trigger itself. The absence of a hardware trigger in the $\bar{P}ANDA$ experiment calls for a different means to ensure proper synchronisation. To this end, a dedicated clock source using a protocol called SODANET over optical fibers is being used, that provides synchronisation to the data concentrators, which then redistribute the clock signal to the digitisers. The SODANET clock has a jitter of about

[3] As can be seen from Figure 2, the recovery of pile-up pulses is limited. If the second pulse follows the first one within the rise time (about 50 ns), the two pulses will appear as one.

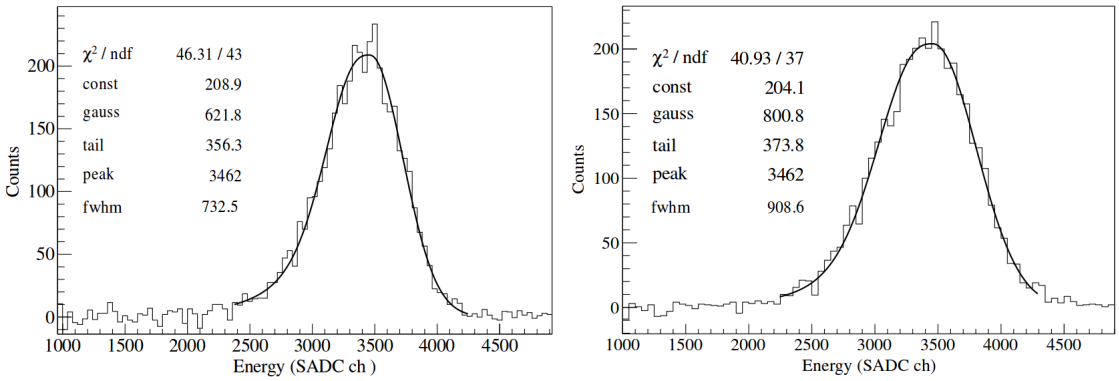

Figure 4. Recovered pile-up pulses, by taking the first peak as A_1 (left), and the second peak as A_1 (right). The figure is taken from [7].

20 ps and continuously monitors the propagation time of the clock signal, compensating for fluctuations when neccesary.

3.5. Compute Nodes

The final event selection takes place in the Compute Nodes. Before data is sent to them, it is sorted in the so-called Burst Building Network. This network collects information belonging to the same time period from the data concentrators of all subsystems, making complete event information for this period available to the Compute Nodes. This information is sent to one of the FPGAs on the Compute Nodes for event selection. In the example of section 2, requiring the invariant mass of combinations of two photons to lie at the pion mass eliminates any background containing η particles (as the mass of the η particle is much higher), and requiring the combined invariant mass of all final state particles to have a peak at 4260 MeV eliminates more background channels. Only events that satisfy these constraints will be sent to storage for offline processing and analyses. By using techniques such as these, a data reduction factor of about 10^3 is expected to be achieved (for all physics channels of interest), leaving 200 MB/s being sent to storage.

4. Status of hardware development

As of the moment of this writing, there are working prototypes for all parts of the readout chain, with the performance of these devices close to their required ones. The firmware, with almost complete functionality, is developed for the digitisers, data concentrators and clock-distribution network (SODANET). The hardware for the EMC digitisers is in the final stage of development, but for the data concentrators, a redesign is neccesary to increase the speed of the optical links.

Implementation and comprehensive testing of an online version of the pile-up recovery algorithm has to be done, as this has only been tested offline, and the topology of the Burst Building Network needs to be optimised. For the latter, a good understanding of the expected data flow is required.

5. Simulating the Data Flow

In order to determine the requirements for the detector components and evaluate the performance of the reconstruction algorithms, an accurate simulation of the expected data flow is needed. The following discussion focusses on the EMC, but most statements hold for other subsystems as well.

In a typical simulation, an event is generated, which then creates several energy depositions in the EMC crystals, called hits. After this, the next event is generated, along with its associated hits, after which this process is iterated. Each generated event is essentially independent of the previous one. The $\bar{P}ANDA$ experiment has to deal with very high interaction rates of 20 MHz, leading to individual crystal hit rates in excess of 500 kHz in the most forward region, creating pile-up of hits from different events in the detector. Furthermore, protons and antiprotons are composite particles, allowing a direct production of a large variety of secondary particles with different lifetimes. Furthermore, the different detector subsystems also have different response times. This will increase the probability for hits of one event overlapping with those from another further. Hence, it makes sense to adjust the simulation procedure accordingly, switching from this sequential (also referred to as "event-based") simulation type to one which takes pile-up into account. This is called a "time-based" simulation.

5.1. The Time-based Simulation

For the time-based simulation, first, a data set is generated as described above. Then, the timestamps of the hits are reassigned, creating pile-up between events; an impression of which is shown in Figure 5. The reconstruction algorithms will need to disentangle this data stream,

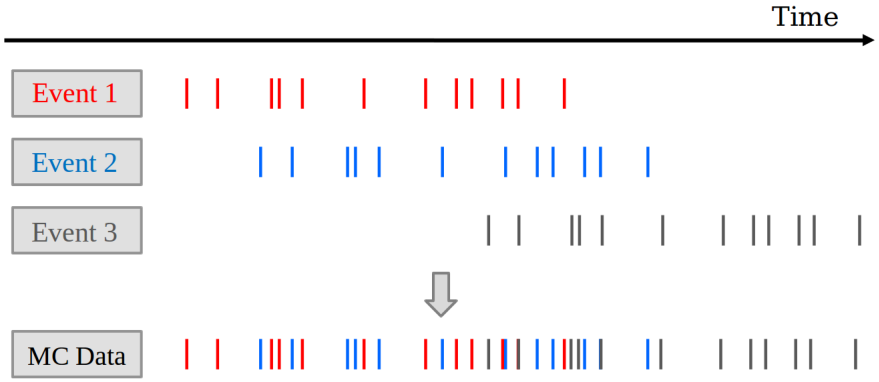

Figure 5. Artist's impression of the generation of the time-based MC data flow. *Courtesy:* T. Stockmanns, FZ Juelich, 2014.

taking pile-up and geometrical overlap into account. Figure 5 shows that the data stream can be cut into bunches in time. Apart from being forward-boosted, particle decays will essentially be isotropic, implying that it is very unlikely for hits from different events within such a time bunch to end up in the same part of the detector, allowing to separate events in space.

This presumption needs testing. The particle shower created by particles hitting the EMC crystals will in general spread out through several of them, creating groups of hits, called clusters. The hits in these clusters will need to be recombined in order to find the particle that spawned the shower. This is called cluster finding, or clustering, for short. An algorithm to perform this task is currently under development by the author, but a preliminary version already shows, using the MC thruth information, that only about 1% of these clusters contain hits from different events. A large number of low energy split-off 'clusters' (mostly consisting of a single hit) was observed, likely contributing to the "contamination" of the clusters. Such low energy split-offs occur when one of the particles in the particle shower scatters out of the crystal and into a neighbouring one. This is often a next-to-nearest neighbour, as low energy particles have a larger mean free path in the scintillation material.

The current tests were done using mono-energetic, 1 GeV photons. The next step would be

to check to performance of the algorithm for a more realistic case, involving particles with multiple photons in the final state, e.g.

$$\bar{p}p \rightarrow h_c \rightarrow \eta_c\gamma \rightarrow \pi^0\pi^0\eta\gamma \rightarrow 7\gamma.$$

Once the simulation tests are successful, the algorithm will be implented into an FPGA for testing in an experiment with one of the EMC prototypes.

6. Summary

This paper discussed the new triggerless readout concept that is envisioned for the future $\bar{P}ANDA$ experiment. This new type of readout is needed because $\bar{P}ANDA$ will have a very high interaction rate, and because the topology of the final-state particles is very similar for the decay channels of interest and its associated background channels, rendering the conventional approach for data reduction unusable.

For the same reason, the simulation of the data flow also required adaptations. The time-based simulation takes into account the effects of pile-up, i.e. when hits of different events start to overlap. An algorithm for clustering, currently under development, is part of the solution to disentangling the resulting data flow.

References

[1] Beringer J *et al* (Particle Data Group) 2012 *Phys. Rev.* D **86** 010001
[2] Liu X 2014 An overview of XYZ new particles *ArXiv* 1312.7408
[3] PANDA Collaboration 2012 Targets technical design report *http://www-panda.gsi.de/html/reports.php*
[4] Keshelashvili I 2014 Development of Low Noise/Low Power Preamplifier for the readout of inorganic scintillators and its mass production test system *This proceedings series*
[5] Wieczorek P and Flemming H 2010 Low noise preamplifier ASIC for the PANDA EMC *IEEE Nucl. Sc. Symp. Conf. Rec. (NSS/MIC)* p1319-22
[6] Kavatsyuk M, Hevinga M, Konorov I, Lemmens P J J, Marciniewski P, Schakel P, Schreuder F, Speelman R, Tambave G *et al* 2011 Trigger-less readout electronics for the PANDA electromagnetic calorimeter *IEEE Nucl. Sc. Symp. Conf. Rec. (NSS/MIC)* p43-47
[7] Tambave G 2013 Electromagnetic calorimeter studies for charmonium physics (PhD thesis - University of Groningen) *http://irs.ub.rug.nl/ppn/356608891*
[8] Tambave G *et al* 2012 Pulse pile-up recovery for the front-end electronics of the PANDA electromagnetic calorimeter *JINST* **7** 11001
[9] Frohlich I, Kajetanowicz M, Korcyl K, Krzemien W, Palka M, Salabura P, Schrader C, Skott P, Strobele H *et al* 2007 A general purpose trigger and readout board for HADES and FAIR-experiments *15th IEEE-NPSS Real-Time Conference* p1-6